ELSEVIER

Computer Communications 20 (1997) 1280–1291

computer communications

Output process characterization for fast token ring networks supporting two priorities

Mingfu Li, Zsehong Tsai*

Department of Electrical Engineering, Rm. 543, National Taiwan University, Taipei, Taiwan

Received 7 October 1996; revised 13 March 1997; accepted 14 May 1997

Abstract

A performance model for the fast token ring connected to an output link via a switching node is considered. For each station, traffic streams of two priority classes are supported. Poisson packet arrival process, Erlang-K packet length distribution and zero walk time are assumed. The output process of one fast token ring with a switching node is characterized by using a 3-phase Markov Modulated Erlang Process (MMEP). The numerical results indicate that the required output link capacity predicted by this approximated process can be much less than the estimation based on the Poisson Process assumption, provided that the congestion at the switching node is kept at the same level. © 1997 Elsevier Science B.V.

Keywords: Fast token ring; Output process characterization; Markov modulated process

1. Introduction

In order to increase the number of stations and to extend the covered area, local area networks closely located are often interconnected by gateways or switching nodes. Since internetwork messages for a token-ring or token-passing LAN [1–3] need to pass through the bridge/switching node, the latter can easily become the network bottleneck. Early studies on interconnected token ring networks and their congestion behavior are available in Refs. [4,5]. One of the most basic problems in analyzing such interconnected systems is the characterization of the output process of a local area network. Such issues have been treated in Refs. [6–9]. Takine et al. [6] considered the polling system with a single buffer at each station. They obtained the output process at each station. This result was then applied to the throughput and mean waiting time analyses of an interconnected polling system which consists of several homogeneous stations with single buffers and a depot station (switch) with infinite buffer. In Ref. [7], Bernoulli and first-order Markov processes were used to approximate the output process of a class of slotted multiuser random access communication networks. In Ref. [8], the idea of approximating the output process of slotted multiuser random access communication networks by a 2nd-order Markov process was introduced. In Ref. [9], the Markov packet train traffic characterization was used to represent the output traffic from a token-ring network when modeling network interconnection. Although all these research results in Refs. [4–8] are of interest in studying LAN interconnection, none of them have considered the priority access operations. It is clear that performance issues of interconnected LANs which involve priority traffic have so far attracted little attention. For example, in the performance analysis of token ring network, significant efforts have been dedicated to the message delay analysis of the single class traffic environment [10,11]. Only a limited number of studies are related to priority access schemes [12–15]. Facing the emerging demand of multi-media communications in the local environment, we believe this is an area requiring further studies.

In this paper, we consider a system where a fast token ring network operating at 100 Mbps with only two priority classes is connected to one full-duplex link by a switching node (or gateway). The switch provides two separate buffers for each transmission direction. To achieve high throughput, the switch performs only simple routing and store-and-forward functions, but not involved in error or flow control. As in most switches, the filtering and forwarding rates are sufficiently high, while the full-duplex link operates at a lower speed. Therefore, comparing the switch processing time with the link transmission time for the packet, we find that the network bottleneck should be at the switch

* Corresponding author. Tel: 886-2-3635251; 886-2-3625252 Ext. 543; Fax: 886-2-3638247; E-mail: ztsai@cc.ee.ntu.edu.tw.

PII S0140-3664(97)00107-2

output link, such that the performance of the switching node is essential to the proper operation of the interconnected network. By assuming Erlang-K packet length distribution, Poisson packet arrivals for both classes, and negligible ring latency time, we use a 3-phase Markov Modulated Erlang Process (MMEP) to approximate the output process of one fast token ring. Since in this 3-phase MMEP, traffic streams of both priority classes are characterized, we are able to employ the 3-phase MMEP as the arrival process of the switching node for a more precise performance analysis.

The organization of the paper is as follows. In Section 2 we describe the assumptions of our model and the justifications for these assumptions. In Section 3 we present an MMEP model for the output process of a fast token ring network and analyze the busy periods on the ring. In Section 4 we analyze the switch performance. In Section 5 we provide several numerical examples. Finally in Section 6 we present our conclusions.

2. Model description

The fast token ring considered here is assumed to contain g infinite buffer stations and one finite buffer switching node with buffer size N. Note that in such a network, the traffic load at each station is usually relatively small as compared with the traffic load at the switching node and hence packet arrivals are rarely lost at a station. So we make the infinite buffer assumption for each station. Next, we assume the packet arrival processes at the ith station ($1 \leq i \leq g$) to follow the Poisson processes with arrival rates λ_{iH} and λ_{iL} for high and low priority packets, respectively. The packet arrival processes from other LANs to the switching node via the transmission link are also assumed to be Poisson processes with rates λ_{0H} and λ_{0L} for high and low priority packets, respectively. The packet service time distributions for both priority classes at each station are assumed to be identical and independent Erlang-K distributions with mean b. Throughout this paper, we assume that the total traffic load $\rho = (\lambda_H + \lambda_L)b < 1$, where $\lambda_H = \sum_0^g \lambda_{iH}$ and $\lambda_L = \sum_0^g \lambda_{iL}$ in order to ensure that the system is stable. Usually, the walk time can be assumed to be negligible when local area networks are considered. Therefore, we make a zero-walk time assumption. On the output link, the packet service times are also assumed to be identical and independent Erlang-K random variables with mean K/μ for both priority packets. At last, we let γ_H and γ_L be the probabilites of high and low priority packets in each station being routed to the switching node (i.e. inter-traffic). Under the above assumptions, one can model the switching node on a fast token ring as a single server queue with non-preemptive priority service discipline. For multi-priority traffic, the arrivals from the ring to the switching node will be a superposition of several packet streams with general interarrival time distributions and the output link can be modeled as the switch server. So the general queueing model at the switching node is a $\Sigma_i G_i/E_K/1/N$ non-preemptive priority queue.

As to the medium access protocol, we employ a procedure almost identical to IEEE 802.5 [2], except that only two priority classes are supported. According to the standard, when a token arrives at one station, the station will capture the token and transmit its packets if the priority levels of those packets are not lower than that of the token. Otherwise, the station only makes reservation on the token if it has packets to be transmitted, or just passes the token to the next station. When certain station captures the token and begins transmitting packets, high priority packets may arrive at other stations. Then reservations can be made for these new arrivals on the transmission packet header in order to determine the priority level of the next issued token. In IEEE 802.5, the reservation field resides in the transmission packet header. If we neglect the propagation delay and the bit latency at each station, we have a system in which the stations with packets at the beginning of the current packet transmission could instantly reserve their transmission rights on the reservation field. In addition, the station which raises the token priority should downgrade the priority of the token at the appropriate time so that low priority packets can be transmitted. In summary, the only difference from IEEE 802.5 is that in this paper we allow the priority and the reservation of a new token to be determined at the beginning of a packet transmission, regardless of any high priority arrival at the current station during the packet transmission.

By setting the token holding time differently, various dwell-time service disciplines can be employed on a token ring. In our model, the service discipline at all stations are set to be limited-1, assuming that the token holding time has been set to the minimal for supporting delay sensitive multimedia communications.

3. Process characterization

In this section, we present the characterization procedure for the departure process of a fast token ring network, which is just the arrival process at the switching node. In the first subsection, we approximate the departure process as a 3-phase MMEP. Then we deduce the transition rates of the MMEP model in terms of key system parameters. In the second subsection, we use the busy period analysis to obtain all the transition rates required in the process characterization.

3.1. The 3-phase MMEP

The queueing model of an output link at the switching node is a generic $\Sigma_i G_i/E_K/1/N$ queue, where the interarrival time of the ith traffic class is of a general distribution. However, several assumptions and approximations are required to make the analysis of such queueing model more mathematically tractable. Therefore, an MMEP/E_K/1/N

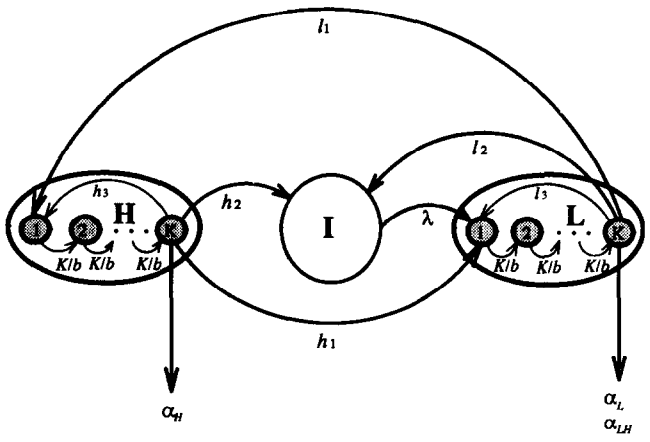

Fig. 1. The MMEP transition diagram.

model is used in this paper. That is, the superposition of G_i streams is approximated by the MMEP. For the fast token ring network with only two priority traffic classes, one 3-phase MMEP model can be defined using the phase set $\{H,L,I\}$, where the phase H indicates the ring to be in the busy period with high priority token, L represents the ring in the busy period with low priority token, and I denotes the idle state at the token ring network. Indeed, according to the IEEE 802.5, in phase I the token priority is low. Since the service time distribution is Erlang-K type, we use K subphases, indexed from 1 to K, to model the service stages in phases H and L.

We now employ the 3-phase MMEP model as an approximation of the packet arrival process at the switching node. Fig. 1 shows the MMEP transition diagram. In the Kth subphase of phase H, high priority packets arrive with a rate equal to α_H, following a Poisson process, but low priority packet arrivals do not occur. In the Kth subphase of phase L, both high and low priority packets arrive according to Poisson processes with rates equal to α_{LH} and α_L respectively. In phase I, since the ring is idle, neither high nor low priority packets will arrive. Note that when the ring is idle, the first arrived packet which changes the ring state from idle to busy should capture the low priority token and begin its transmission, independent of its priority class. Therefore, there is no transition probability from phase I into phase H. Furthermore, since we assume high and low priority packets to arrive at a token ring according to the Poisson processes with total rates λ_H, λ_L respectively, the idle period duration of the ring is an exponential random variable with mean $(\lambda_H + \lambda_L)^{-1}$. As a result, the transition rate from phase I into phase L is equal to $\lambda = \lambda_H + \lambda_L$. Based on these facts, the generator matrix for denoting the transition rates among phases $\{H,L,I\}$ is given by

$$\mathbf{T} = \begin{bmatrix} -(h_1+h_2) & h_1 & h_2 \\ l_1 & -(l_1+l_2) & l_2 \\ 0 & \lambda & -\lambda \end{bmatrix}$$

In the following, we derive the parameters which are needed for our MMEP arrival process model. Once they are obtained, we can then proceed to the performance analysis of the switching node. From Fig. 1, one can show that the probabilities of all subphases in phase $H(L)$ are the same by the global balance equations. Thus, one can readily obtain

$$(h_1+h_2)\frac{P_H}{K} = l_1\frac{P_L}{K} \tag{1}$$

$$(l_1+l_2)\frac{P_L}{K} = h_1\frac{P_H}{K} + \lambda P_I \tag{2}$$

where P_H, P_L, and P_I are, respectively, the probabilities that the system lies in phases H, L, and I in steady state. Obviously, $P_H + P_L + P_I$ is equal to 1 and $P_I = 1 - \rho$. In addition, one can easily derive the mean sojourn times of the phases H, L, and I to be given by:

$$\overline{H} = \frac{K}{h_1+h_2} \tag{3}$$

$$\overline{L} = \frac{K}{l_1+l_2} \tag{4}$$

$$\overline{I} = \frac{1}{\lambda} \tag{5}$$

where H is the random variable representing the length of the busy period with high priority token; L is the random variable indicating the length of the busy period with low priority token; and I is the random variable denoting the length of the idle period.

Solving Eqs. (1)–(4), we have

$$l_1 = \frac{KP_H}{P_L\overline{H}} \tag{6}$$

$$l_2 = \frac{K}{\overline{L}} - \frac{KP_H}{P_L\overline{H}} \tag{7}$$

$$h_1 = \frac{KP_L}{P_H\overline{L}} - \frac{KP_I\lambda}{P_H} \tag{8}$$

$$h_2 = \frac{K}{\overline{H}} - \frac{KP_L}{P_H\overline{L}} + \frac{KP_I\lambda}{P_H} \tag{9}$$

On the contrary, we also observe from the detailed balance equation for the state of the Kth subphase in phase L or H and conclude that the following equations hold.

$$h_1+h_2+h_3 = \frac{K}{b},$$

$$l_1+l_2+l_3 = \frac{K}{b}$$

Hence, by Eqs. (3) and (4), we can derive

$$h_3 = \frac{K}{b} - \frac{K}{\overline{H}}, \tag{10}$$

$$l_3 = \frac{K}{b} - \frac{K}{\overline{L}} \tag{11}$$

Next, since the mean service times of high and low priority packets are both equal to b, and by the flow conservation law during phases H and L, the parameters α_H, α_L, and α_{LH} must satisfy the following equations:

$$\frac{K}{b} = \frac{\alpha_H}{\gamma_H}\left(\frac{\lambda_H}{\sum_{i=1}^{g}\lambda_{iH}}\right), \tag{12}$$

$$\lambda_H = \left(\frac{\alpha_{LH}P_L}{\gamma_H K} + \frac{\alpha_H P_H}{\gamma_H K}\right)\left(\frac{\lambda_H}{\sum_{i=1}^{g}\lambda_{iH}}\right), \tag{13}$$

$$\frac{K}{b} = \frac{\alpha_L}{\gamma_L}\left(\frac{\lambda_L}{\sum_{i=1}^{g}\lambda_{iL}}\right) + \frac{\alpha_{LH}}{\gamma_H}\left(\frac{\lambda_H}{\sum_{i=1}^{g}\lambda_{iH}}\right) \tag{14}$$

Consequently, the expressions for α_H, α_L and α_{LH} are given by

$$\alpha_H = \left(\frac{\sum_{i=1}^{g}\lambda_{iH}}{\lambda_H}\right)\frac{\gamma_H K}{b}, \tag{15}$$

$$\alpha_{LH} = \left(\frac{\sum_{i=1}^{g}\lambda_{iH}}{\lambda_H}\right)\frac{K(\lambda_H b - P_H)\gamma_H}{bP_L}, \tag{16}$$

$$\alpha_L = \left(\sum_{i=1}^{g}\lambda_{iL}\right)\frac{K\gamma_L}{P_L} \tag{17}$$

Once the values of $\overline{H}$, $\overline{L}$, P_H, P_L, and P_I are determined, one can calculate all the parameters for the MMEP model by Eqs. (6)–(11) and Eqs. (15)–(17). We now proceed to derive approximation formulas for these parameters using busy period analysis.

3.2. Busy period analysis

In the following analysis, we found that it is easier to derive $\overline{H}$ by first modifying the service discipline used in phase L. Since the order of packet transmission within phase L does not affect the sojourn time at phase H, the derived result for $\overline{H}$ should hold under the original scheme. The detailed analysis of H busy period is left to Appendix A.

Next, we will derive a formula for the mean value of the period L. The system time can be a combined sequence of H, L, and I periods as shown in Fig. 2, where it shows the only two possible cases between two subsequent high priority token periods H. When the system is in steady state, P_I, the probability of the token ring being idle, is equal to $(1-\rho)$. For ergodic processes, one can look at the probability P_S as the percentage of time in the steady state that the system is in phase S, where $S = H, L, I$. Thus, one can show that

$$P_H = \frac{\overline{H}}{\overline{H} + \overline{T_L}} \tag{18}$$

$$P_I = \frac{\overline{N_I}\,\overline{I}}{\overline{H} + \overline{T_L}} \tag{19}$$

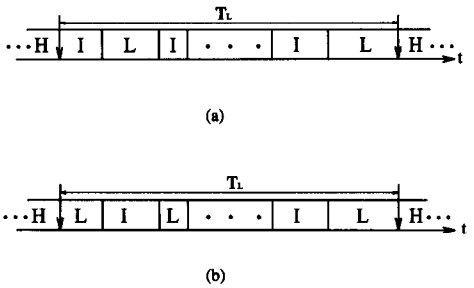

Fig. 2. Two possible sequences of I–L periods between two subsequent periods H.

where T_L is the length of the period between two subsequent high priority token periods H; and N_I is the number of idle periods in a period corresponding to T_L. In deriving Eq. (19), we have used the Wald's equation to obtain the average length of total idle periods between two subsequent high priority token periods. For the phase sequences shown in Fig. 2, we let the probabilities that the period H followed by I and L be denoted as P_a and P_b, respectively. Obviously, $P_a + P_b$ must be equal to 1. Since $p_d(0)$ (see Appendix A), the probability that there is no high priority packet at the end of phase H, is close to 1 for most traffic conditions and P_a is equal to the probability that the system is idle at the packet departure instant in phase H, one can approximate P_a as the probability that the system is idle at the packet departure instant given that there are no high priority packets in the system. Thus, we can use the approximation

$$P_a = \frac{1-\rho}{1-\rho_H}, \tag{20}$$

$$P_b = \frac{\rho_L}{1-\rho_H}, \tag{21}$$

where ρ_L is the utilization of the token for low priority packets and is equal to $\lambda_L b$. Moreover, the probabilities that the system will change to phase I and phase H at the packet departure instant, given the system in phase L, are approximated by $(1-\rho)$ and P_h, respectively, where P_h (see Appendix A) is equal to the probability that an arbitrary packet transmission in phase L leads to a phase transition to phase H. The transition probability from phase L into phase H is thus equal to

$$P_{LH} = \frac{P_h}{P_h + (1-\rho)}$$

Now, $\overline{N_I}$ can be calculated from the following equation:

$$\overline{N_I} + P_b = \frac{1}{P_{LH}}$$

Using Eq. (19), we can obtain $\overline{T_L}$ as follows:

$$\overline{T_L} = \frac{\overline{N_I}\,\overline{I}}{1-\rho} - \overline{H} \tag{22}$$

One can also observe from Fig. 2 and apply Wald's equation to obtain

$$\overline{T_L} = (\overline{N_I} + P_b)\bar{L} + \overline{N_I}\,\bar{I} \tag{23}$$

Hence, we have the following formula:

$$\bar{L} = \frac{\overline{T_L} - \overline{N_I}\,\bar{I}}{\overline{N_I} + P_b} \tag{24}$$

All the parameters that will be employed for the analysis of an MMEP/E_K/1/N model are now available. During the above derivation, we find that packet length distributions other than Erlang-K can also be employed, and thus this approximation procedure is not constrained by the Erlang-K packet length assumption.

4. Performance analysis of the switching node

We are now ready to analyze the performance of the switching node, which is equivalent to solve the stationary state probabilities for an MMEP/E_K/1/N non-preemptive priority queue. In order to solve the problem, we define $\{(n(t),i(t),j(t),k(t),s(t),u(t)),\ t \geq 0\}$ as the system state process and $P(n,i,j,k,s,u)$ as the stationary state probability, where the state (n,i,j,k,s,u) is defined as follows.

- n: total number of packets in the queue $0 \leq n \leq N$,
- i: the phase in which the state lies, and we let i be equal to 0,1 and 2 for phases H, L and I, respectively,
- j: the number of low priority packets waiting in the buffer, $0 \leq j \leq n-1$, and $j = 0$ if $n = 0$
- k: the service class, if $n = 0$ then $k = 0$, otherwise k is set to be 1 and 2 for high and low priority packets in service, respectively,
- s: the service stage, $s = 1,2,\ldots,K$ for $n > 0$ and $s = 0$ for $n = 0$,
- u: the subphase index in phase H or L, $u = 1,2,\ldots,K$ for $i = 0,1$ and $u = 0$ for $i = 2$.

From the above definitions, it can be shown that $(n(t), i(t), j(t), k(t), s(t), u(t))$ is a Markov process. Besides, it can be easily derived that the total number of states is $d(N, K) = (2K + 1)[KN(N + 1) + 1]$. Thus, we introduce the vector

$$\mathbf{\Pi} = [\pi_1, \pi_2, \cdots, \pi_{d(N,K)}]$$

in which $\pi_z = P(n,i,j,k,s,u)$, where

$$z = \begin{cases} iK + u & \text{if } n = 0,\ i = 0,1 \\ 2K + 1 & \text{if } n = 0,\ i = 2 \\ d(n-1,K) + (2ni + 2j + k - 1)K^2 + (s-1)K + u & \text{if } n > 0,\ i = 0,1 \\ d(n-1,K) + 4nK^2 + (2j + k - 1)K + s & \text{if } n > 0,\ i = 2 \end{cases}$$

According to the above specification, the generator matrix for the system state process, denoting as $\mathbf{Q}$ can be obtained. It is a block tridiagonal matrix and satisfies the following equations

$$\mathbf{QI} = \mathbf{0},\ \mathbf{\Pi Q} = \mathbf{0},\ \mathbf{\Pi 1} = 1 \tag{25}$$

where $\mathbf{1}$ represents the vector $[1,1,\ldots,1]^T$ with dimension $d(N, K)$.

Unfortunately, the matrix-geometric approach used in Refs. [16] and [17] for solving regular MMPP /G/1/N queue cannot be directly applied here since the blocks of submatrices in $\mathbf{Q}$ are not of the same size, due to the priority service discipline. However, such a set of linear equations can still be solved efficiently using the Crout Factorization (see Ref. [18]) for a block tridiagonal matrix, even when the total number of states is large.

Once $P(n, i, j, k, s, u)$ is obtained by Eq. (25) and a corresponding $\mathbf{Q}$ matrix, various performance measures can be calculated. For example, the mean queue length, mean queueing delay, throughput, and packet loss probabilities can be derived as follows.

Let the mth moment of the queue length for high and low priority packets be denoted as $Q^m(h)$ and $Q^m(l)$, respectively. They can be shown to be given by

$$Q^{(m)}(h) = \sum_{n=1}^{N} \sum_{j=0}^{n-1} \sum_{i,k,s,u} (n - 1 - j)^m P(n,i,j,k,s,u), \tag{26}$$

$$Q^{(m)}(l) = \sum_{n=1}^{N} \sum_{j=0}^{n-1} \sum_{i,k,s,u} j^m P(n,i,j,k,s,u) \tag{27}$$

A similar approach can be applied to the packet loss probabilities for high and low priority packets, which are represented as $P_l(h)$ and $P_l(l)$, respectively. The loss probability is equal to the total packet losses divided by the total packet arrivals. Since high priority packet arrivals occur in both phases H and L, the total loss of high priority packets is equal to the sum of losses in phases H and L. Similarly, the total arrivals include the arrivals in phase H and the arrivals in phase L. Thus, $P_l(h)$ can be represented as follows.

$$P_l(h) = \frac{\sum_{j=0}^{N-1} \sum_{k,s} \{\alpha_H P(N,0,j,k,s,K) + \alpha_{LH} P(N,1,j,k,s,K)\}}{\sum_{n=0}^{N} \sum_{j=0}^{n-1} \sum_{k,s} \{\alpha_H P(n,0,j,k,s,K) + \alpha_{LH} P(n,1,j,k,s,K)\}} \tag{28}$$

Since the arrivals for low priority packets only occur in phase L, one can express $P(l)$ as

$$P_l(l) = \frac{\sum_{j=0}^{N-1} \sum_{k,s} P(N,1,j,k,s,K)}{\sum_{n=0}^{N} \sum_{j=0}^{n-1} \sum_{k,s} P(n,1,j,k,s,K)} \tag{29}$$

The link throughput for high and low priority traffic, $S(h)$ and $S(l)$, can be derived as follows.

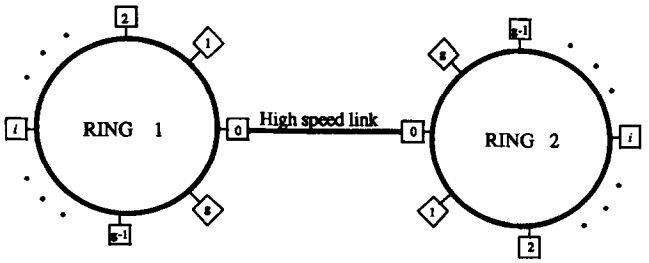

Fig. 3. The interconnected token ring network model.

$$S(h)=\sum_{n=0}^{N-1}\sum_{j=0}^{n-1}\sum_{k,s}\{\alpha_H P(n,0,j,k,s,K) + \alpha_{LH}P(n,1,j,k,s,K)\} \quad (30)$$

$$S(l)=\sum_{n=0}^{N-1}\sum_{j=0}^{n-1}\sum_{k,s}\alpha_L P(n,1,j,k,s,K) \quad (31)$$

By applying Little's Formula, the mean queueing delay for high and low priority packets, $D(h)$ and $D(l)$, can be easily obtained as follows.

$$D(h)=\frac{Q^{(1)}(h)}{S(h)} \quad (32)$$

$$D(l)=\frac{Q^{(1)}(l)}{S(l)} \quad (33)$$

5. Numerical results

In this section, we consider the network environment that two symmetrical fast token rings are interconnected by two switches (or gateways) and one full-duplex link, as shown in Fig. 3. We use the analytical results presented in previous sections to evaluate the performance of the switching nodes in such a network environment. Meanwhile, simulation results are also depicted to demonstrate our analytical results. During simulation, the external Poisson packet traffic streams are set according to the analytical model. Meanwhile, the output process of a remote switch is employed as the arrival process from the remote ring to the local ring. A constant non-zero walk time is also chosen. The parameters used in the simulation are specified as follows. The transmission rate is 100 Mbps for the two fast token rings. The mean packet length is 4.5 Kbytes for both priority classes. The walk time is constant and is set equal to 1 μs.

In the first example, on each ring we assume 10 stations, each with $\lambda_i = 0.2$ packets per ms, while γ_H and γ_L are set to be identical and range from 0.035 to 0.14. Packet service times Erlang-2 distributed. The switching node buffer size is set to be 10 and the transmission link is of the speed 8.448 Mbps (E2). In Fig. 4, the mean queue length at the switching node versus the total link traffic load is shown. And the mean queueing delay is plotted in Fig. 5. We observe that our analytical results coincide with the simulation statistics. In Fig. 5, it indicates that the mean queueing delay of high priority packets at the switching node is much smaller than 10 miniseconds as long as the traffic is not overloaded. We thus believe that the fast token ring is capable of carrying real time multimedia traffic. Although the mean queue length and the mean queueing delay for the two priority classes are quite different, we found that the packet loss probabilities are almost the same for high and low priority packets, as shown in Fig. 6. This is due to the fact that we employed a shared buffer management policy at the

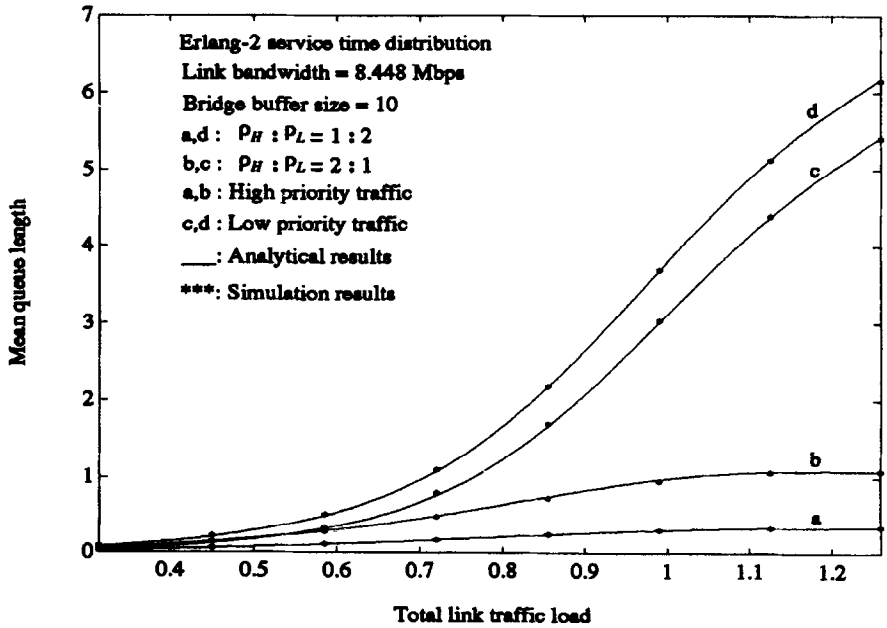

Fig. 4. The mean of the queue length at the switching node ($g = 10$; $\lambda_i = 0.2$ packets per ms, $i = 1\sim10$; $\gamma_H = \gamma_L = 0.035\sim0.14$.

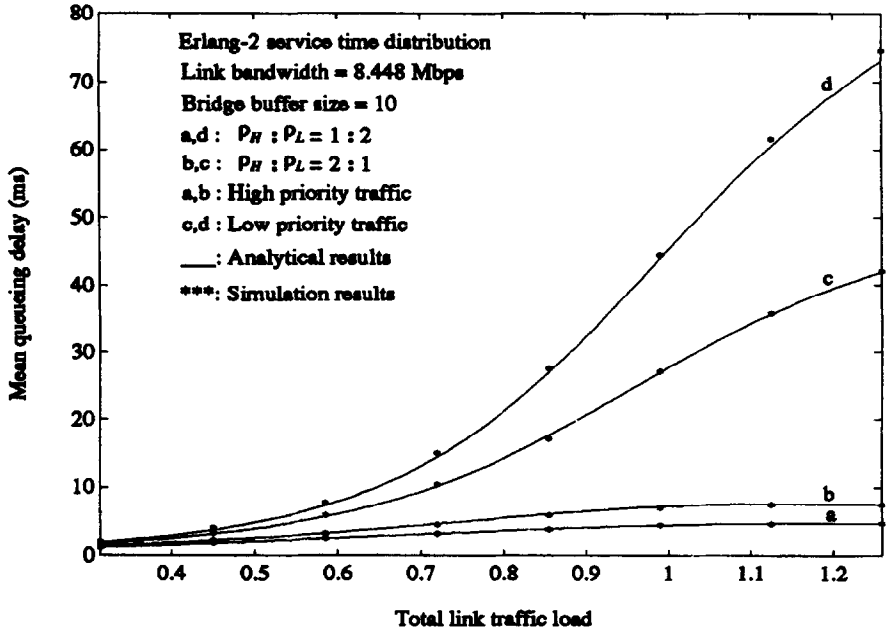

Fig. 5. The mean queueing delay at the switching node ($g = 10$; $\lambda_i = 0.2$ packets per ms, $i = 1 \sim 10$; $\gamma_H = \gamma_L = 0.035 \sim 0.14$).

switching node. Namely, if one wishes to have different packet loss probabilities for high and low priority traffic, different buffer allocation schemes must be considered. For example, partial buffer sharing, pust-out scheme, etc., could be employed. Under different buffer sharing schemes, we only need to change the generator matrix **Q** slightly and then follow the same analytical methods as described in previous sections. The behavior of throughput versus total link traffic load is plotted in Fig. 7. When the traffic load is light, packet losses nearly occur and the throughput increases linearly with the traffic load. However, if the load is heavy, the congestion will be serious at the switching node and packet losses occur frequently. The throughput will eventually approach the link bandwidth and cannot increase any more. All the above results indicate that our MMEP model can accurately characterize the output process of a fast token ring.

In the following, we use two examples to compare the accuracy of our results with that of the regular Poisson assumption. Here, we allocate 10 stations on each ring, with $\lambda_i = 0.15$ ($i = 1 \sim 10$) packets per ms. In Fig. 8, the mean queue length at the switching node is shown. It

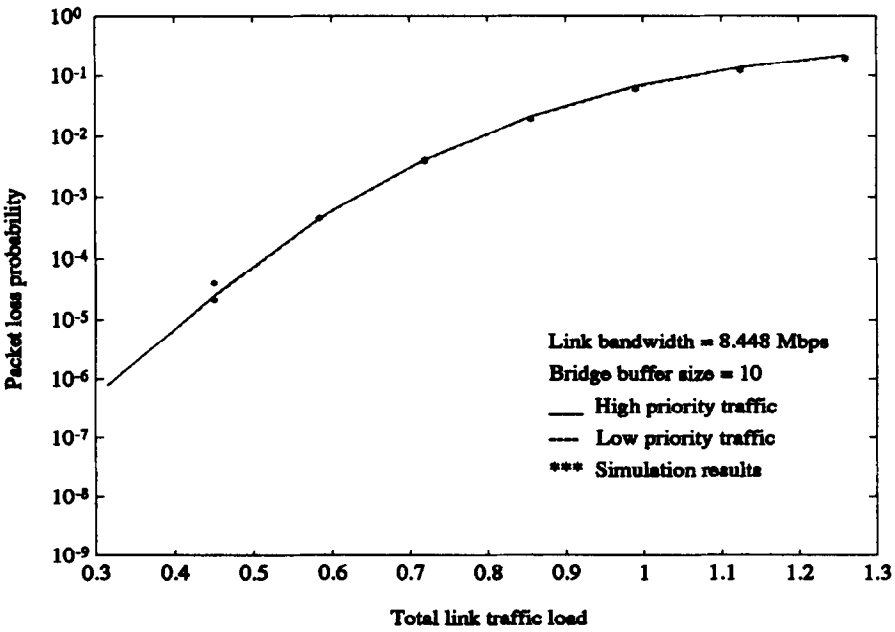

Fig. 6. Packet loss probability at the switching node versus total link traffic load ($g = 10$; $\lambda_i = 0.2$ packets per ms, $i = 1 \sim 10$; ρ_H: $\rho_L = 1 : 2$; $\gamma_H = \gamma_L = 0.035 \sim 0.14$).

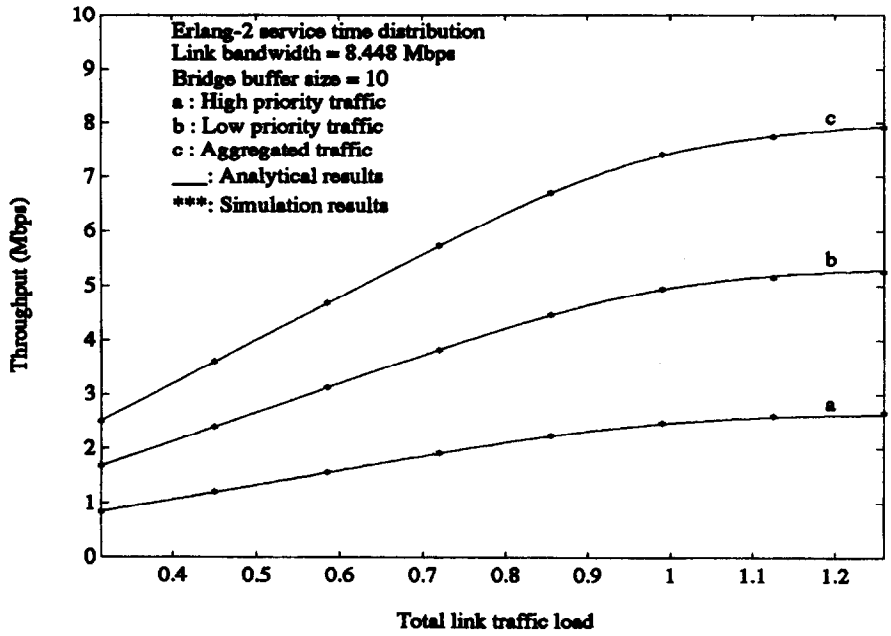

Fig. 7. Throughput at the switching node versus total link traffic load ($g = 10$; $\lambda_i = 0.2$ packets per ms, $i = 1 \sim 10$; $\rho_H : \rho_L = 1 : 2$; $\gamma_H = \gamma_L = 0.035 \sim 0.14$).

illustrates that the mean queue length can be overestimated by using the regular Poisson arrival process when the link speed is changed to 100 Mbps. While the analytical results of our MMEP model can accurately coincide with the simulation results. We thus conclude that our MMEP model is much better than the Poisson assumption in modeling the departure process of a token ring network. In order to further understand the causes of such differences, another example is considered. In Fig. 9, the mean queue length under different link bandwidth, obtained from our MMEP model as well as the Poisson model, are compared with the simulation results. When the link bandwidth varies, we keep the link traffic load at 0.25 by changing γ_H and γ_L. It is obvious that the accuracy of the Poisson assumption degrades rapidly as the link bandwidth increases. In turn, the MMEP model should have reflected more correlation among the interdeparture time than the simple Poisson model. Hence, the MMEP model can accurately characterize the departure process under a wide range of link bandwidth.

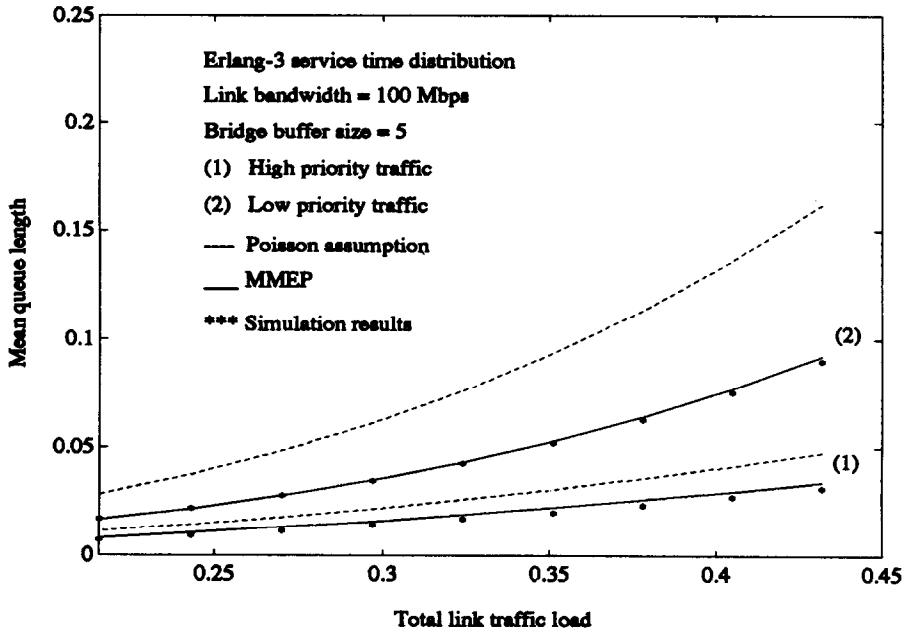

Fig. 8. The mean queue length at the switching node ($g = 10$; $\lambda_i = 0.15$ packets per ms, $i = 110$; $\rho_H : \rho_L = 1 : 2$; $\gamma_H = \gamma_L = 0.4 \sim 0.8$).

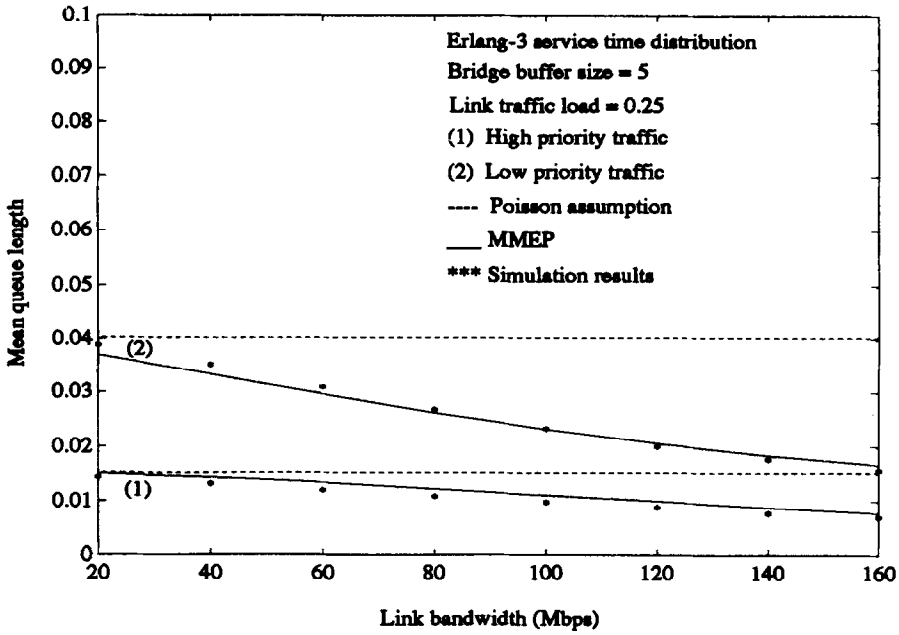

Fig. 9. The mean queue length at the switching node versus different link bandwidth ($g=10$; $\lambda i=0.15$ packets per ms, $i=1\sim10$; $\rho_H:\rho_L=1:2$; $\gamma_H=\gamma_L=0.0926\sim0.741$).

6. Conclusions and future extensions

Considering the behavior of a fast token ring network supporting two priorities, we have characterized its output process in an internetworking environment. We have then used this process, which is equivalent to the inflow process at the switching node, to analyze the switch performance. The numerical results presented in this paper suggest that the MMEP is an excellent approximation to the output process of a priority-based fast token ring network. Our results can be readily applied to the engineering of link capacities on the backbone of a corporate network, especially when multi-media traffic is introduced. With our approach, the predicted mean queue length at the switch output can be much less (and more accurate) than that obtained under Poisson assumption, as the speed of LAN interconnection link increases. Consequently, the engineering of output link capacity is strongly suggested to assume the 3-phase MMEP instead of Poisson process, either in the mathematical analysis or in a simulation procedure when high speed out-going ports are employed. One should note that the presented approach is not limited to the Erlang-K service time assumption since the MMEP model is just a special case. When the actual packet length is of other distribution, this model can still be applied by using a moment matching technique.

It is also possible to extend this model to the performance studies of other high speed networking solutions. As long as the high-speed LAN involved similar transitions between high and low priority busy periods, this model can also be applied. For example, for a 100VG- AnyLAN [19] network supporting multimedia traffic, one can match the busy periods of high and low priority packet transmissions with

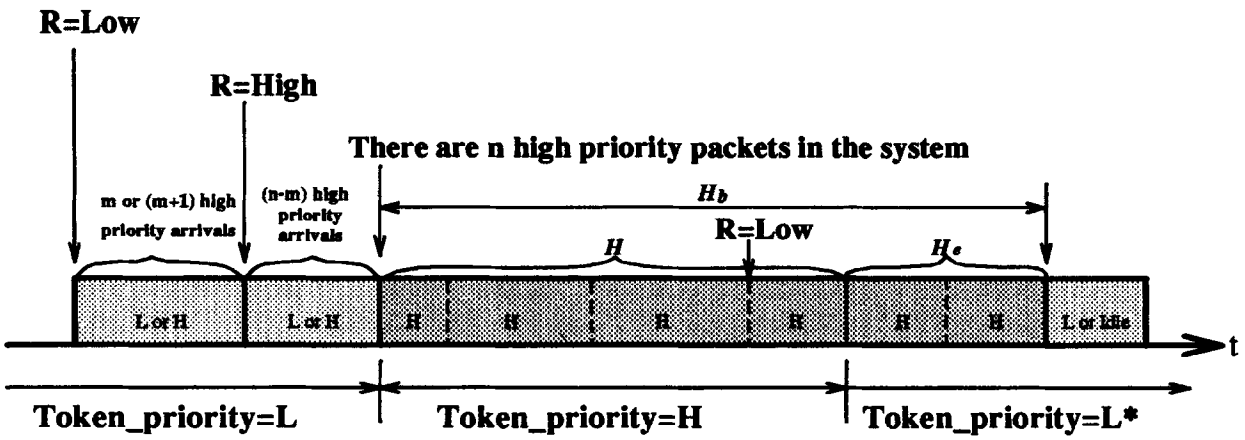

Fig. 10. The relationship of periods H, H_b and H_e in the packet transmission sequence, where R = High/Low indicates the reservation priority. During the L* period, the service discipline is modified as described in Section 3.2.

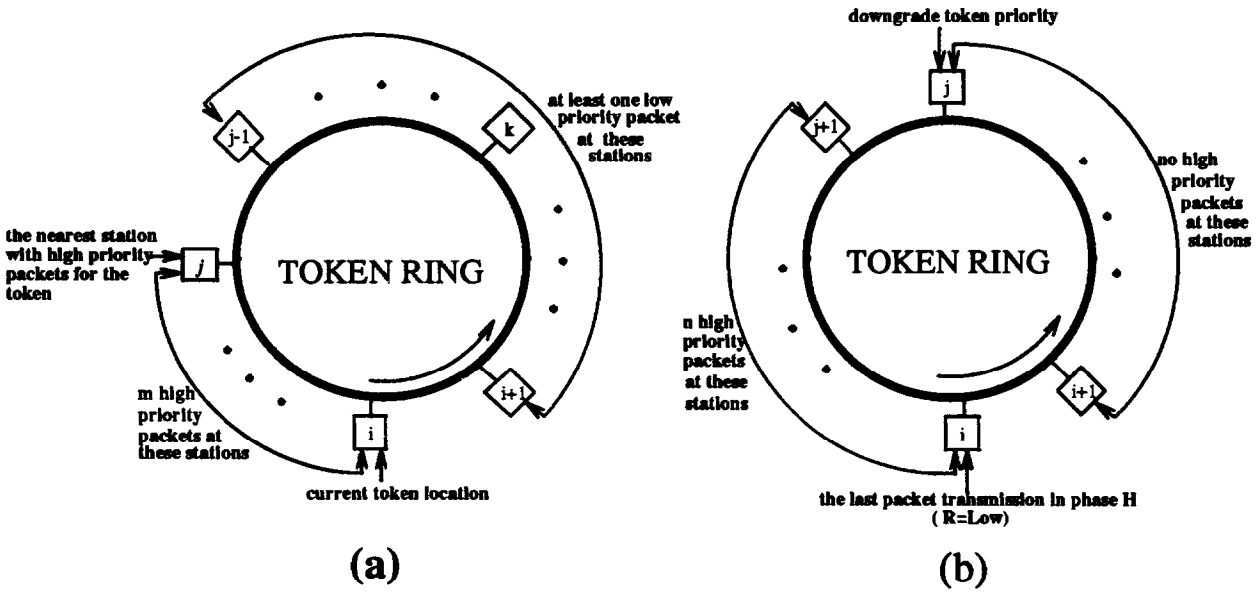

Fig. 11. Illustrations for the conditions used to derive a_m and $p_d(n)$. (a) condition in which a low priority packet will be served next, while m high priority packets are present. (b) Condition in which the token priority is downgraded while n high priority packets are present.

the phases H and L in the MMEP model and derive a similar 3-phase MMEP model for its output process. The congested repeater in a 100VG-AnyLAN can be modeled as the switching node. Only the transition parameters and the mean busy periods of H and L in the MMEP model should be re-calculated via analysis or moment matching. This would be the future work.

Acknowledgements

This work was supported in part by National Science Council of the Republic of China under Grant NSC81-0408-E-002-05 and NSC82-0416-E-008-083.

Appendix A: Busy period analysis of H

Our approach assumes the service discipline to be as follows. During phase H, the service order of high priority packets and the reservation scheme are the same as the described in Section 2. When the system is in phase L, the service order of high and low priority packets is set the same as an FCFS non-preemptive 2-priority queue, regardless of the packet location. Therefore, we can express the random variable H as follows.

$$H = H_b - H_e$$

where H_b is the random variable indicating the busy period of high priority packet transmission starting from the beginning of phase H to the end of the transmission for all high priority packets on the ring, and H_e is the random variable denoting the sub-busy period of high priority packet transmission resulting from the high priority arrivals during the last packet service time in phase H. One should note that the sub-busy period length H_e can be of zero length when there is no high priority packet on the ring at the end of phase H. The relationship of H, H_b, and H_e is depicted in Fig. 10. Now, we are ready to obtain $\overline{H_b}$ and $\overline{H_e}$.

For a regular *M/G/1* queueing system with packet arrival rate λ_H, it is well known that $H_1^*(s)$, the Laplace–Stieltjes Transform (LST) of the busy period H_1, is characterized by

$$H_1^*(s) = B^*[s + \lambda_H(1 - H_1^*(s))], \tag{34}$$

where $B^*(s)$ is the LST of $B(t)$ which is the CDF of the packet service time distribution. It is easy to show that

$$H_n^*(s) = [H_1^*(s)]^n, \tag{35}$$

where $H_n^*(s)$ is the LST of the random variable H_n which denotes the length of the busy period starting with $n (n \geq 1)$ packets. Therefore, the LST of the random variable H_b can be obtained from the following equation.

$$H_b^*(s) = \sum_{n=1}^{\infty} p_n H_n^*(s), \tag{36}$$

where p_n is the probability that there are n high priority packets in the system at the beginning instant of phase H. Since the priority and the reservation of a newly issued token is determined at the beginning of a packet transmission, the number of high priority arrivals during the previous two packet service time determines p_n (see Fig. 10). Thus, it

is given as below:

$$p_n = \frac{1}{P_h}\sum_{m=1}^{n}\left\{a_m\int_0^\infty \frac{(\lambda_H t)^m}{m!}e^{-\lambda_H t}dB(t) + (1-a_{m+1})\int_0^\infty \frac{(\lambda_H t)^{m+1}}{(m+1)!}e^{-\lambda_H t}dB(t)\right\} \times \int_0^\infty \frac{(\lambda_H t)^{n-m}}{(n-m)!}e^{-\lambda_H t}dB(t) \quad (37)$$

The first (second) term in the summation accounts for the condition that the packet served just before phase H is a low (high) priority packet. The parameter a_m is the probability that the low priority packet will be served next, given that there are m high priority packet arrivals during the present service time in phase L (see Fig. 11(a)), and it follows the approximation:

$$a_m = \sum_{i=0}^{g}\frac{\lambda_i}{\lambda}\sum_{j=i+2}^{i}\left\{\left(\sum_{k=j}^{i}\frac{\lambda_{kH}}{\lambda_H}\right)^m - \left(1-\sum_{k=i+1}^{j}\frac{\lambda_{kH}}{\lambda_H}\right)^m\right\}\left\{\left(1-\prod_{k=i+1}^{j-1}(1-\lambda_{kL}\bar{c}_{ik})\right)\right\}, \quad (38)$$

where $\{1-\Pi_{k=i+1}^{j-1}(1-\lambda_{kL}\bar{c}_{ik})\}$ is the probability that at least one low priority packet resides among stations $(i+1)$ to $(j-1)$ for some i and j, and $\{(\sum_{k=j}^{i}\frac{\lambda_{kH}}{\lambda_H})^m - (1-\sum_{k=i+1}^{j}\frac{\lambda_{kH}}{\lambda_H})^m\}$is the probability of m high priority packets present at stations with indices from j to i and at least one high priority packet residing at station j. The indices i, j are the relative location on the ring and $\sum_{k=j}^{i} = \sum_{k=j}^{g} + \sum_{k=0}^{i}$ if $i < j$. $\bar{c}_{ik}$ is the conditional mean cycle time in phase L, given that there is a packet served at station i and no packets served between stations $(i+1)$ to $(k-1)$. Under stable network condition, $\bar{c}_{ik}$ can be approximated as

$$\bar{c}_{ik} = b + \sum_{j\neq i,\cdots,k-1} b\{[1-B^*(\lambda_{jH})] + B^*(\lambda_{jH})\lambda_{jL}\bar{c}_{ik}\}, \quad (39)$$

where $[1-B^*(\lambda_{jH})]$ is the probability of at least one high priority packet arrival at station j during one packet service time, and $B^*(\lambda_{jH})\lambda_{jL}\bar{c}_{ik}$ is the probability of no high priority packet arrival at station j during one packet service time and at least one low priority packet arrival at station j during $\bar{c}_{ik}$. Subsequently, $\bar{c}_{ik}$ can be expressed as

$$\bar{c}_{ik} = \frac{b + b\sum_{j\neq i,\cdots,k-1}[1-B^*(\lambda_{jH})]}{1-\sum_{j\neq i,\cdots,k-1}B^*(\lambda_{jH})\rho_{jL}}, \quad (40)$$

where $\rho_{jL} = \lambda_{jL}b$. The normalization factor P_h in Eq. (37) is equal to the probability that an arbitrary packet transmission in phase L leads to a phase transition to phase H, and is expressed as

$$P_h = 1 - B^*(\lambda_H) - (1-a_1)\int_0^\infty \lambda_H t e^{-\lambda_H t}dB(t) \quad (41)$$

Substituting Eqs. (37) and (38) into Eq. (36), we obtain

$$H_b^*(s) = \frac{B^*(z)}{P_h H_1^*(s)}\left\{B^*(z) - H_1^*(s)(1-a_1)\int_0^\infty \lambda_H t e^{-\lambda_H t}dB(t) - B^*(\lambda_H)\right\} + \frac{B^*(z)}{P_h}\left[1-\frac{1}{H_1^*(s)}\right]\sum_{i=0}^{g}\frac{\lambda_i}{\lambda}\sum_{j=i+2}^{i} \times \left\{1-\prod_{k=i+1}^{j-1}(1-\lambda_{kL}\bar{c}_{ik})\right\} \times \left\{B^*\left[\lambda_H - \sum_{k=j}^{i}\lambda_{kH}H_1^*(s)\right] - B^*\left[\lambda_H - \left(\lambda_H - \sum_{k=i+1}^{j}\lambda_{kH}\right)H_1^*(s)\right]\right\}, \quad (42)$$

where $z = \lambda_H - \lambda_H H_1^*(s)$.

Similarly, we can derive $H_e^*(s)$, the LST of the random variable H_e, from the equation

$$H_e^*(s) = \sum_{n=0}^{\infty} p_d(n)H_n^*(s), \quad (43)$$

where $p_d(n)$ is the probability that there are n high priority packets at the end of phase H (see Fig. 11(b)), and it is given by

$$p_d(n) = \frac{1}{p_d}\sum_{i=0}^{g}\frac{\lambda_{iH}}{\lambda_H}\sum_{j=0}^{g}\frac{\lambda_j}{\lambda}\left(\sum_{k=j+1}^{i}\frac{\lambda_{kH}}{\lambda_H}\right)^n\int_0^\infty \frac{(\lambda_H t)^n e^{-\lambda_H t}}{n!}dB(t) \quad (44)$$

Since the probability of upgrading the token priority at each station is nearly proportional to the number of packet transmissions at this station, in Eq. (44) we have approximated the probability that the token priority is downgraded by station j with λ_j/λ. It can be readily shown that

$$H_e^*(s) = \frac{1}{p_d}\sum_{i=0}^{g}\frac{\lambda_{iH}}{\lambda_H}\sum_{j=0}^{g}\frac{\lambda_j}{\lambda}B^*[\lambda_H - \sum_{k=j+1}^{i}\lambda_{kH}H_1^*(s)] \quad (45)$$

where

$$p_d = \sum_{i=0}^{g}\frac{\lambda_{iH}}{\lambda_H}\sum_{j=0}^{g}\frac{\lambda_j}{\lambda}B^*(\lambda_H - \sum_{k=j+1}^{i}\lambda_{kH}).$$

The above equations hold for any $B^*(s)$. For the special case that service time distribution is Erlang-K, $B^*(s)$ is of the form

$$B^*(s) = \frac{(K/b)^K}{(s+K/b)^K},$$

and one could derive the equality

$$\int_0^\infty \lambda_H t e^{-\lambda_H t}dB(t) = \frac{\rho_H}{(1+\rho_H/K)^{K+1}}$$

where ρ_H is the utilization of the token for high priority packets and is equal to $\lambda_H b$. After taking the derivatives

of $H_b^*(s)$, $H_e^*(s)$, and setting s to zero, we can easily obtain $\overline{H_b}$ and $\overline{H_e}$. Hence, the formula for approximating $\overline{H}$ is given by

$$\overline{H} = \frac{\overline{H_1}}{P_h}\sum_{i=0}^{g}\frac{\lambda_i}{\lambda}\sum_{j=i+2}^{i}\left\{1-\prod_{k=i+1}^{j-1}(1-\lambda_{kL}\overline{c_{ik}})\right\}$$
$$\times\left\{\left(1+\sum_{k=i+1}^{j-1}\frac{\rho_{kH}}{K}\right)^{-K}-\left(1+\sum_{k=i+1}^{j}\frac{\rho_{kH}}{K}\right)^{-K}\right\}$$
$$+\frac{\overline{H_1}}{P_h}\left\{\rho_H-\frac{(1-a_1)\rho_H}{\left(1+\frac{\rho_H}{K}\right)^{K+1}}\right\}-(1-\rho_H)\overline{H_1}$$
$$-\overline{H_1}\sum_{i=0}^{g}\frac{\lambda_{iH}}{\lambda_H}\sum_{j=0}^{g}\frac{\lambda_j}{\lambda}\left(\sum_{k=j+1}^{i}\rho_{kH}\right)$$
$$\times\left(1+\frac{\rho_H}{K}\sum_{k=j+1}^{i}\frac{\rho_{kH}}{K}\right)^{-(K+1)} \quad (46)$$

where $\rho_{kH}=\lambda_{kH}b$ and $\overline{H_1}=b/(1-\rho_H)$. In the derivation of Eq. (34) to Eq. (46), we found that our additional assumption for the service discipline in phase L does not affect the result for $\overline{H}$ but simplifies the analysis.

References

[1] Institute of Electrical and Electronics Engineers, Token-Passing Bus Access Method and Physical Layer Specifications. IEEE Standard 802.4, 1989.

[2] Institute of Electrical and Electronics Engineers, Token Ring Access Method and Physical Layer Specifications. IEEE 802.5, 1989.

[3] American National Standards Institute, Fiber Distributed Data Interface (FDDI)—Token Ring Media Access Control (MAC). ANSI X3.139, 1987.

[4] W. Bux, D. Grillo, Flow control in local-area networks of interconnected token rings, IEEE Trans. Commun. 33 (10) (1985) 1058–1066.

[5] O.C. Ibe, X. Cheng, Analysis of Interconnected Systems of Token Ring Networks, Comp. Commun. 13 (3) (1990).

[6] T. Takine, Y. Takahashi, T. Hasegawa, Performance analysis of a polling system with single buffer and its application to interconnected networks, IEEE J. Select. Areas Commun. 4 (6) (1986) 802–812.

[7] I. Stavrakakis, D. Kazakos, On the approximation of the output process of multiuser random-access communication networks, IEEE Trans. Commun. 38 (2) (1990) 172–178.

[8] I. Stavrakakis, D. Kazakos, Performance analysis of a star topology of interconnected networks under 2nd-order Markov network output processes, IEEE Trans. Commun. 38 (10) (1990) 1724–1731.

[9] E.M. Spiegel, C. Bisdikian, A.N. Tantawi, Characterization of the traffic on high-speed token-ring networks, Performance Evaluation 19 (1994) 47–72.

[10] H. Takagi, Analysis of Polling Systems, The MIT Press, 1985.

[11] H. Takagi, Queueing analysis of polling models, ACM Comp. Survey 20 (1) (1988) 5–28.

[12] J. Gianini, D.R. Manfield, An analysis of symmetric polling systems with two priority classes, Performance Evaluation 5 (1988) 93–115.

[13] B. Grela-M'Poko, M.M. Ali, J.F. Hayes, Approximate analysis of asymmetric single-service prioritized token passing systems, IEEE Trans. Commun. 39 (7) (1991) 1037–1040.

[14] Z. Tsai, I. Rubin, Performance of token schemes supporting delay-constrained priority traffic streams, IEEE Trans. Commun. 38 (1990) 1994–2003.

[15] H. Saito, M. Kawarasaki, H. Yamada, An analysis of statistical multiplexing in an atm transport network, IEEE J. Select. Areas Commun. 9 (3) (1991) 359–368.

[16] W. Fisher, K. Meier-Hellstern, The Markov-modulated poisson process (MMPP) cookbook, Performance Evaluation 18 (1992) 149–171.

[17] M. F. Neuts, Matrix-Geometric Solutions in Stochastic Models: An Algorithmic Approach, Johns Hopkins, Baltimore and London, 1981.

[18] G. H. Golub, C. F. Van Loan, Matrix Computations, 2nd Edn., Johns Hopkins, Baltimore and London, 1989.

[19] IEEE Standards Department, Draft Standard—Information Technology—Local and Metropolitan Area Networks—Part 12: Demand-Priority Access Method, Physical Layer and Repeater Specifications for 100 Mb/s Operation—Draft 6.0, 23 November, 1994.

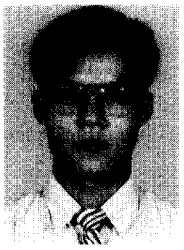

Mingfu Li was born in Miaoli, Taiwan, Republic of China, in 1968. He received the B.S. degree in electrical engineering from the National Taiwan University in 1991. Since 1991, he has been a graduate student in the Department of Electrical Engineering at the National Taiwan University where he is currently a Ph.D. candidate. His current research interests include high performance LAN protocols, traffic shaper design and analysis, congestion control and deterministic performance evaluation in ATM networks.

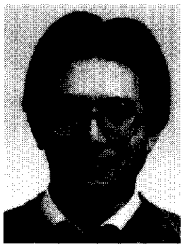

Zsehong Tsai received the B.S. degree in electrical engineering from the National Taiwan University, Taipei, in 1983, and the M.S. and Ph.D. degrees from the University of California, Los Angeles, in 1985 and 1988, respectively. During 1988–1990, he worked as a Member of Technical Staff at AT&T Bell Laboratories, where he investigated performance aspects of network management systems. Since 1990 he has been an Associate Professor in the Department of Electrical Engineering of the National Taiwan University. Currently he is also with the Graduate Institute of Industrial Engineering and the Center of Telecommunications Research at the National Taiwan University.

Dr Tsai was responsible for technical support for the ATM testbed deployment, cross-campus ATM internetworking trials, and a cross-Pacific satellite ATM trial at the NAtional Taiwan University. His research interests include high speed networking, wireless communications, network management, and performance evaluation of telecommunication networks. He is also a member of IEEE and ACM.